# Simple Stochastic Model of Multiparticle Battery Electrodes Undergoing Phase Transformations

Norman C. Bartelt, Yiyang Li, Joshua D. Sugar, Kyle Fenton, A. L. David Kilcoyne, David A. Shapiro, Tolek Tyliszczak, William C. Chueh, and Farid El Gabaly

Phys. Rev. Applied **10**, 044056 — Published 24 October 2018

DOI: 10.1103/PhysRevApplied.10.044056

# A simple stochastic model of multi-particle battery electrodes undergoing phase transformations

Norman C. Bartelt[1], Yiyang Li[2], Joshua D. Sugar[1], Kyle Fenton[3], A. L. David Kilcoyne[4], David A. Shapiro[4], Tolek Tyliszczak[4], William C. Chueh[2], and Farid El Gabaly[1]

[1]Sandia National Laboratories, Livermore, CA 94550

[2]Materials Science and Engineering, Stanford University, Stanford, CA 94305

[3]Sandia National Laboratories, Albuquerque, NM 87123

[4]Advanced Light Source, Lawrence Berkeley National Laboratory, Berkeley, CA 94720

**Abstract**

Incorporation of ions into battery electrodes can lead to phase transformations. When multi-particle phase-transforming electrodes charge or discharge, two processes must occur in each particle: the new phase must nucleate, and then grow until the particle is fully charged or discharged. A fundamental question is which of these two processes is rate limiting. Here we construct a simple stochastic model that shows how the relative rate of nucleation compared to growth determines the particle state-of-charge distributions in the electrode. We find that the number of particles that are partially charged at any time increases as the relative nucleation rate increases. The maximum number of particles that are actively charging occurs just before the time when the first particles are becoming completely charged. By comparing measured state-of-charge distributions to the model, the relative rate of nucleation can be determined. We apply this procedure to measurements of the evolution of particles in $LiFePO_4$ cathodes and show we can account for the particle state-of-charge distribution as a function of the electrode state of charge.

## Introduction

A thorough understanding of how battery electrodes charge at a microscopic level will be ultimately crucial to improving their macroscopic performance. For example, in multi–particle electrodes, a crucial question is how many particles are charging or discharging at any particular time. Small numbers of actively charging particles can lead to locally high current densities and degrade battery performance. Consequently, several techniques have recently been developed to image the nanoscale evolution of electrodes [1-4]. These experiments can be difficult to interpret in terms of distinct atomic processes because the diffusion of electrons/ions, charge transfer kinetics at interfaces, and phase transformations all must be understood thoroughly in chemically complex materials that can be far from equilibrium. Usually these quantities are not individually directly accessible to the experiments. A promising approach that has recently been taken is to compare experiment with comprehensive electrode models [4-6]. But still it is a challenge to isolate the effects of particular atomic processes on the configuration of an electrode.

Our goal in this paper is to provide a simple baseline model to which experimental data can be compared. We focus solely on the mechanisms of nucleation and growth in two-phase multi-particle electrodes, even though it is likely that other processes are also important in any real electrode. The problem to be solved is, given snapshots in time of the charging process, how can information about the relative importance of nucleation and growth be extracted? For example, how does the number of actively charging or discharging particles depend on how fast nucleation occurs?

In multi-particle phase transforming electrodes, nucleation and growth are competitive processes. Initially a fully charged battery electrode has all particles in the same state. The first step is that a new phase must nucleate in some of the particles. This nucleation is a stochastic, random process that can be specified by some overall rate (which in classical nucleation theory can be associated with some critical nucleus size). Once the new phase nucleates, further transformation can occur by motion of the phase boundary within the particle. Both the boundary velocity and nucleation rate depend on the charging current, as well as the number of particles transforming. Because the number of transforming particles changes with time, a non-trivial problem arises. It is not possible to predict the microscopic configuration of the electrode at one point in time, by just specifying a discharge current at that time. For example, there can be many particles with slow moving boundaries or a few particles with fast moving ones. Because this configuration depends on the past history of the electrode, one must model the complete time evolution, starting from the untransformed state. As we will show below, a requirement of such a model is that it must consider the *distribution* of the state of charge of the actively charging particles. We find that the time dependence can be captured by a single parameter, the ratio of nucleation rate to growth rate. (The kinetics model proposed by Bai and Tian [7] although very similar in spirit to ours, does not include such effects of the particle state of charge distribution.) As an illustration of the use of our model, we compare its predictions to observations of cathodes consisting of $LiFePO_4$ (LFP) particles, the prototypical example of a system in which lithiation involves a phase transformation.

**Stochastic model of particle filling**

We first assume that the battery electrode consists of $N$ identical particles. We model the situations in which the charging or discharging rate is constant. Each particle is taken to have a capacity of $L$ units of charge. In a particular unit of time a set amount of charge or discharge will occur. We chose this time interval to correspond to adding or subtracting one unit of charge. Initially all of the particles are assumed to be empty. In the first time interval one charge unit (e.g., a lithium ion or lithium vacancy) is added to a randomly chosen particle. Thereafter there are two choices for the added charge unit. Either it is added to an empty particle (i.e., nucleation occurs) or to a partially filled one (i.e., a phase boundary is moved). $P_{\text{empty}}$ is the probability that the charge unit is added to an empty particle, while $P_{\text{active}}$ is the probability it is added to a partially filled one. The assumption of constant charging rate dictates $P_{\text{empty}}+P_{\text{active}}=1$. If there were no extra barrier to nucleating, $P_{\text{empty}}$ and $P_{\text{active}}$ would be equal to the fraction of empty or partially filled particles, respectively. With a nucleation barrier, there will be additional proportionality factors $a_1$ and $a_2$ that bias against adding to empty particles:

$$P_{\text{empty}} = \frac{a_1 N_{\text{empty}}}{N_{\text{empty}} + N_{\text{active}}}, \quad (1)$$

and

$$P_{\text{active}} = \frac{a_2 N_{\text{active}}}{N_{\text{empty}} + N_{\text{active}}}. \quad (2)$$

The ratio $r = \frac{a_1}{a_2}$ is a measure of the difference of the barriers for nucleation and boundary motion; r < 1 if a nucleation barrier exists. For simplicity we assume *r* does not depend on time. These equations implicitly assume that only one nucleation event occur per particle. Given $r$, the values of $a_1$ and $a_2$ are determined by the requirement that $P_{\text{empty}}+P_{\text{active}}=1$.

The consequences of this model on the particle filling dynamics can be readily computed with a Monte Carlo simulation. For purposes of illustration, we choose $N = 10000$ and $M = 100$, i.e., 10000 particles, each of them with a capacity of 100 units of charge. We start with a cathode which all particles are empty and add charge (i.e., lithium or lithium vacancies) according to the above algorithm, with probabilities generated at each time step using a random number generator. Figure 1 shows the population of empty, partially filled and full particles as a function of total electrode state of charge for various choices of $r$. If $r$ is very small (i.e., nucleation is difficult compared to boundary motion), as in Fig. 1(a), the number of active particles is always very small, approaching one in the limit of vanishing $r$. This is the "particle-by-particle" limit described in Ref. [8]. As $r$ increases as shown in Figs. 1(b-d), the number of active particles becomes larger throughout the discharge process. In the limit of large $r$ (Fig. 3(e)), all of the particles become active. This is the "concurrent intercalation" limit of Ref. [8].

It is important to note that the number of active particles changes during the discharge, and reaches a maximum $N_{\text{active}}^{\max}$ at a certain intermediate state of charge, $q$. By examining the $q$ dependence of the number of filled particles plotted in Fig. 1, it is evident that this maximum corresponds to when the first particles are becoming full. In the "particle-by-particle" limit, particles become full immediately – the time to discharge a single particle is much smaller than the time to discharge the entire cathode. As $r$ increases, the "incubation time" becomes larger. In the limit of large $r$, the time to fill a particle becomes comparable to the cathode discharge time.

To explain this behavior, and give explicit expressions for $N_{\text{active}}^{\max}$ and the incubation time in terms of physical properties, we now develop the model analytically in the limit of large *N* and *L*. To analytically describe the problem, we divide the time evolution of the transforming electrode into two parts: before and after the first particle becomes filled. Before that moment, there will only be empty and active particles competing. We will then proceed to calculate the moment the first particle becomes filled. Finally, we will calculate the distribution of active and filled particles at every state of charge.

At the early stages of discharge, the cathode has only empty and active particles. From Eqs. (1) and (2), the probability to add charge to an empty particle is

$$P_{\text{empty}} = r\, N_{\text{empty}}/(N_{\text{active}} + rN_{\text{empty}}). \quad (3)$$

Since no particle has had time to fill $N_{\text{active}} + N_{\text{empty}} = N$. In this regime

$$P_{\text{empty}} = r\, N_{\text{empty}}/(N - (1-r)\, N_{\text{empty}}). \tag{4}$$

When the unit of charge $dQ$ added at each step is infinitesimally small compared to $L$ and $N$, we can write

$$P_{\text{empty}} = -\frac{d}{dQ} N_{\text{empty}}.$$

Combined with Eq. (4) this gives a differential equation for $N_{\text{empty}}$:

$$\left(N - (1-r) N_{\text{empty}}\right) \frac{d}{dQ} N_{\text{empty}} = -r\, N_{\text{empty}}. \tag{5}$$

From the boundary condition the $N_{\text{empty}}(Q = 0) = 0$ and using the fact that Lambert-W function [9], defined by $W(y)e^{W(y)} = y$, is the solution of $y(1+W)dW/dy = W$ one finds:

$$N_{\text{empty}}(Q) = -\left[\frac{N}{1-r}\right] W\left[-(1-r)e^{-\left(1-r+\frac{rQ}{N}\right)}\right]. \tag{6}$$

This result is of course only valid when there are no filled particles.

To express Eq. (6) in terms of a macroscopically measurable quantity, we introduce the dimensionless parameter $\alpha = rM$. In terms of the time scales of particle filling, $\alpha$ can be straightforwardly interpreted as:

$$\alpha = \frac{\tau_{\text{fill}}}{\tau_{\text{nucleate}}}, \tag{7}$$

where $\tau_{\text{fill}}$ is the time (at some particular state of charge) to fill a particle after nucleation and $\tau_{\text{nucleate}}$ is the corresponding average time between nucleation events. Or, equivalently, in terms of rates:

$$\alpha = \frac{k_{\text{nucleation}} L}{v}, \tag{8}$$

where $k_{\text{nucleation}}$ is the nucleation rate at some time and $v$ is the phase boundary velocity at the same time, and $L$ is a linear dimension of the particle.

We propose that the parameter $\alpha$ is a useful way of quantifying the behavior of phase transforming electrodes. It provides a qualitative way of predicting how the particle populations change with charging/discharging conditions. For example, nucleation rate generally depends more strongly on the overpotential than the growth velocity [10]. So as charging/discharging

rates are increased, one expects, from Eq. (7), that $\alpha$ will increase, leading to a larger number active particles. This provides a simple explanation of the observations in Ref. [8].

In the limit of large M (i.e. when the unit of charge added to a particle is much smaller than the total capacity of a particle) we can take the limit $r \to 0$, with α fixed. In terms of the state of charge of the entire multiparticle electrode $q = Q/NM$, Eq. (6) then becomes

$$\frac{N_{\text{filled}}}{N} = 0$$

$$\frac{N_{\text{empty}}}{N} = -W[-e^{-(1+aq)}] \tag{9}$$

$$\frac{N_{\text{active}}}{N} = 1 + W\left[-e^{-(1+aq)}\right].$$

To determine that state of charge $q_F$, when particles begin to fill, the rate of boundary motion in individual particles needs to be considered. Since each active particle receives charge with the same probability, in the limit that the amount added to a particle in each step is small compared to the total charge of a particle, all the active particles will receive charge at the same rate $P_{\text{active}}/N_{\text{active}}$. Consequently, the first particles to be filled will be those that are nucleated first. As shown in Appendix A this occurs when the state of charge is

$$q_F = 1 + \frac{e^{\alpha}}{\alpha} - \frac{1}{\alpha}\ . \tag{10}$$

Once particles begin to become full, the number of active particles begins to decrease. This is because at this stage the rate of creation of active particles – i.e. the nucleation rate – is smaller than it was initially, so that the rate at which the active particles fill is greater than the rate at which they are created.

The subsequent evolution of filled, empty, and active particle populations in the electrode after particles begin to become full (i.e., for $q > q_F$), is calculated from the distribution of the state of charge of individual particles. Defining the particle state of charge $q_p$ it is shown in Appendix B that the probability of finding $q_p$ for *all* total *q,* is given by

$$p(q_p) = \frac{\alpha}{e^{\alpha}-1} e^{\alpha q_p}. \tag{11}$$

This constancy of the distribution leads directly to the result (see Appendix C for the derivation) that the number of filled, empty and active particles varies linearly with *q*:

$$\frac{N_{\text{filled}}}{N} = 1 - \frac{\alpha(1-q)e^{\alpha}}{e^{\alpha}-1}$$

$$\frac{N_{\text{empty}}}{N} = \frac{\alpha(1-q)}{e^{\alpha}-1} \qquad (12)$$

$$\frac{N_{\text{active}}}{N} = \alpha(1-q).$$

The maximum number of active particles is therefore

$$N_{\text{active}}^{\max} = \alpha(1-q_F)\,N.$$

The entire evolution for the case of $\alpha = 0.8$ is shown in Fig. 1(f). Comparison with Fig. 1(c) shows that the analytic model accurately reproduces the simulation results. We have numerically confirmed that this analytic model is precise when $N$ and $M$ are very large.

**Comparison with experiment**

Cathodes consisting of (LFP) are an example of a phase transforming system for which the answer to the question of the role of nucleation of new phases is important. In past work we have shown that all the particles of LFP electrodes do not charge or discharge concurrently [3,11]. Only a fraction of the particles at any time are actively charging or discharging. Most of the particles are either single phase $FePO_4$ or $LiFePO_4$. The fraction of active particles becomes smaller when the charge/discharge rate decreases [3,4,8]. We proposed that the qualitative underlying reason for this behavior is a competition between nucleation and growth rates within individual particles. We now compare the model discussed above with experimental results on particle evolution in slowly discharged LFP to show how the model can be used to quantify this competition. Previous studies have presented evidence that there exist other phenomena that might be important in determining the fraction of active particles. For example, nucleation can be so difficult that, the phase transformation is suppressed and charging and discharging occurs through an intermediate metastable solid solution phase [4,12-14]. Li diffusion between particles driven by the minimization of the total area of $FePO_4$ /$LiFePO_4$ phase boundary also can be important [15,16]. Somewhat surprisingly, we can account for the particle evolution in the discharge reaction by assuming this competition is dominant and neglecting the existence of metastable phases and interparticle coarsening.

**Experimental details**

Scanning transmission X-ray microscopy (STXM) and the recent development of ptychography for x-ray microscopy [17] allows for the particle-by-particle characterization of the configuration of LFP electrodes. The chemical state within each particle in a region of an electrode charged to a specified state is mapped as described below.

Sample preparation details have been given in a previous publication, but we will repeat them here for completeness. The electrodes consist of 88 wt% carbon-coated LFP (Mitsui Engineering Shipbuilding), 6 wt% polyvinylidene fluoride (PVDF) and 6 wt% Shawinigan acetylene black carbon. PVDF was first dissolved in N -methyl-2-pyrrolidone. LFP and carbon black were added to the slurry to obtain a viscosity of ∼200 cP. The slurry was then cast onto a carbon-coated aluminum current collector using a reverse comma coater. Solvent was dried at 100 ˚C in ambient and subsequently dried under vacuum at 100 ˚C for ∼12 h. The electrode mass loading and thickness were ∼9 mg $cm^{-2}$ and 60 μm, respectively. Finally, the LFP electrode was assembled in a 2032 coin cell, which consisted of a Li anode, a 50 μm Tonen separator, and 1.2 M $LiPF_6$ in 3:7 (wt/wt) ethylene carbonate/ethyl methyl carbonate electrolyte.

The battery was first operated by initiating five delithiation and lithiation cycles (with rates C/12 and C/6, respectively) with voltage limits of 3.8 V for delithiation and 2.5 V for lithiation. The resulting capacity at this point was ~150 mAh/g. Subsequently, the cell was completely delithiated at rate C/2 and then lithiated at a rate of 5C to $q$ = 42% . After reaching the desired state of charge, to restrain any further processes from occurring the cell was rapidly disassembled and rinsed with excess dimethyl carbonate in a dry room to prevent any further process from occurring. The entire process was completed in less than 4 minutes which is faster than typical voltage relaxation times in $LiFePO_4$ [18,19]. Finally, we used an ultramicrotome to cross-section the $LiFePO_4$ cathode and current collector into 300-nm-thick strips that are thin enough for transmission x-ray microscopy.

STXM at beam lines 11.0.2, 5.3.2.2 and 5.3.2.1 in the Advanced Light Source (LBNL) was used for local state of charge maps (~30 nm resolution) using the Fe $L_3$ x-ray absorption edge. For sub-particle state of charge mapping, we used peak energies of 704 eV for pre-edge, and 707.5 and 710 eV for identification of $LiFePO_4$ and $FePO_4$ phases, with high-resolution ptychography STXM at ~ 10 nm resolution.

Figure 2(a) shows a snapshot of a local configuration of the LFP electrode made using ptychography STXM. The green and red regions represent $FePO_4$ and $LiFePO_4$, respectively. Most of the particles (69%) are entirely composed of one phase. But 31% of the particles are mixed phase, i.e., active. Previous studies could not resolve the nature of the active phase particles [3,8,11]. Fig. 2(a) shows they contain a single sharp phase boundary. We determine the state of charge $q_p$ of each of these actively transforming particles. In Fig. 2(b) we show the histogram of the number of particles at each $q_p$.

As emphasized above, the state of a many particle electrode depends crucially on its past history. So it is essential that our model reproduce the entire state-of-charge dependence of the particle population dynamics. To test this, we performed a least squares fit to Eqs. (9-12) to the active and full particle fractions shown in Fig. 3. We find $\alpha = 0.76$. Clearly the model accounts for all of the observations, which is remarkable, given that only one parameter was adjusted.

Another test of the model is that it reproduces the distribution of the state of charge of the active particles. Fig. 2(b) shows the result of a least-squares fit of the data to Eqs. (11), giving $\alpha = 0.73$, essentially the same value deduced from Fig. 3.

**Discussion**

A factor that we have neglected but that could reduce the number of actively charging particles is interparticle Li transport due to chemical potential gradients [15,16] in the electrode. For example, each phase boundary costs some free energy. Thus in principle there is a Li chemical potential gradient between particles if a flow in Li would reduce total phase boundary area. One way this could happen is if initially nucleated phase boundaries contained more phase boundary per moved Li, than established active particles, causing a flow from less filled particles to more completely filled particles. The signature of such an effect would be fewer active particles with small domains than that given by Eq. (9). Fig. 2(b) shows that there is no such depletion of small domains for LFP and that the state-of-charge distribution can be modeled well assuming that no interparticle transport occurs, at least for the rates of discharge rate of this experiment. Of course, whether interparticle diffusion is significant in general will depend on the overall charging rates.

For large charging rates, X-ray diffraction experiments [12] suggest that nucleation is avoided and instead the particles are in a metastable solid solution state during charge/discharge. If this scenario were to apply to our (lower charging rate) data, the domain boundaries we observe would have developed after the discharge stopped. However, even in the case of charging through a metastable solid solution, our statistical model might be expected to still apply if, as has been proposed [4,8], the rate of filling the solid solution depends on the particle state of charge. In this case, the "activation" barrier" [8] for the initial particle filling would play the role of the nucleation barrier in our model.

The model provides a simple rationalization for the observed asymmetries [8,20] between charging and discharging, since nucleation rates for charging and discharging (and hence $\alpha$) will in general be different because forming phase A in phase B will require different structural rearrangements than B in A. For example, the speed for random thermal fluctuations in Li rich phases will be different that in a Li poor phase because of differences in Li diffusivities.

In real electrodes there will be a distribution of particle sizes. Because smaller particles would fill more quickly, one effect of a distribution of sizes would be to smear out the discontinuous change in particle filling rates that occurs at $q_F$ as smaller particles. Such effects would be compounded if nucleation rates depend strongly on particles size. For example, if small particles nucleated new phases more quickly, the "incubation time" for particle filling would be further reduced. (For LFP, the size dependence on nucleation rates is claimed to be small [3].)

The model also suggests strategies for enhancing the performance of battery electrodes. For example, the high electrical current density within individual particles produces a small number of active particles which might be harmful. However, our model demonstrates that number of active particles depends on the past history of charge/discharge rates. Momentarily increasing

charging rates to increase the number of active particles would, at least temporarily, result in an increased number of active particles and lower current densities during the charge/discharge cycle. Similarly, not completely discharging the electrode before charging could initially increase the number of active particles.

Bai and Tian's earlier model [7] of multi-particle phase transforming particles also emphasizes the importance of the competition between (stochastic) nucleation and phase boundary motion. However, it differs from our model in one crucial respect: Bai and Tian assume (in their Eq. (3)) that the rate of increase of the number of filled particles is simply proportional to the total number of active particles, whereas we, more physically, consider the states of charge of the active particle and take the rate of filling proportional to the number of almost full particles. So for example, Bai and Tian's model would not predict the "incubation time" for the creation of full particles, and cannot be used to compute the charge distribution of Fig. 2(b).

## Conclusion

Our model is an attempt to determine the consequences on multi-particle electrodes of the competition between phase nucleation and phase boundary motion. Since we ignore all diffusive processes that would decrease boundary area after nucleation, our model represents the extreme case where the electrode configuration is determined entirely by the kinetics of particle filling. Equations (9-12) represent the principal result: they describe how the ensemble of particles fill when the charging rate is constant assuming that there is a barrier for nucleating the new phase in each particle. They predict that the maximum number of particles that are actively charging occurs just before the time when the first particles are becoming completely charged.

Increased spatial resolution to < 10nm using ptychography STXM data has confirmed that only a fraction of particles in LFP battery electrodes are active at any one time during charging and discharging. The model quantitatively accounts for the evolution of this active fraction. Somewhat surprisingly, we find that it is unnecessary to invoke interparticle Li diffusion and metastable solid solutions to explain this data.

## Acknowledgements

This work was funded by the Laboratory Directed Research and Development (LDRD) Program at Sandia National Laboratories, a multi-mission laboratory managed and operated by National Technology and Engineering Solutions of Sandia, LLC, a wholly owned subsidiary of Honeywell International Inc., for the U.S. Department of Energy's National Nuclear Security Administration under contract DE-NA-0003525. The research at Stanford was supported by Samsung Advanced Institute of Technology Global Research Outreach program, and by startup funding from Stanford School of Engineering and Precourt Institute for Energy. The Advanced Light Source is supported by the Director, Office of Science, Office of Basic Energy Sciences, of the U.S. Department of Energy under Contract No. DE-AC02-05CH11231. Y. L. was supported by the National Science Foundation Graduate Research Fellowship under Grant No. DGE-

114747. We acknowledge Mark Homer of Sandia for ultramicrotoming.

## Appendix A

To compute the value of the total charge $Q$ of the electrode at the point when particles begin to be filled, we need to determine the state of charge $x_0$ of these first nucleated particles. This is just

$$x_0(Q) = \int_0^Q dQ'\, P_{\text{active}}(Q')/N_{\text{active}}(Q'). \tag{A1}$$

Using $N_{\text{active}} = N - N_{\text{empty}}$ , $P_{\text{active}} = 1 - P_{\text{empty}}$ and Eqs. (4-6), this becomes

$$\begin{aligned} x_0(Q) &= \int_0^Q dQ'\ 1/N(1 + W((-1+r)\, e^{-(1-r+rQ'/N)})) \\ &= \frac{Q}{N} + \frac{1}{r}\left(-W\left((-1+r)e^{(-1+r)}\right) + W\left((-1+r)e^{\left(-1+r-\frac{rQ}{N}\right)}\right)\right) \end{aligned} \tag{A2}$$

Setting $x = M$ and solving for $Q$, gives the total electrode charge $Q_F$ when the first particles begin to be filled:

$$Q_F = NM\left(1 + \frac{e^{-rM}}{rM} - \frac{1}{rM} + \frac{1}{M} - \frac{e^{-rM}}{M}\right),$$

yielding Eq. (11) in the continuum limit of large *M* and small *r* with $q_F = \frac{Q_F}{NM}$.

## Appendix B

To compute the evolution in the electrode after particles begin to become full, we consider the distribution of state of charge of individual particles and define $n(Q,x)dx$ as the number of active particles that have charge between $x$ and $x + dx$. (For a cylindrical particle with nucleation at one end and a phase boundary transverse to its length, $x$ is the distance the phase boundary has propagated, in units of some lattice constant.) The value of $n(Q,x)dx$ at $x = 0$ is determined by the nucleation probability times the number of steps required to move the phase boundary by $dx$, i.e. $dx/\,(P_{\text{active}}/N_{\text{active}})$

$$n(Q,0)dx = P_{\text{empty}}\, dx\, /(P_{\text{active}}/N_{\text{active}}) = N_{\text{empty}}(Q)\, r\, dx$$

or

$$n(Q,0) = N_{\text{empty}}(Q)r. \tag{A3}$$

To compute the number of particles with state of charge $x$, we note that a phase boundary at position $x$ at total charge $Q$ moves to position $x + dQ\ /(P_{\text{active}}/N_{\text{active}})$ when the state of charge is $Q + dQ$:

$$n(Q + dQ, x) = -n\left(Q, x - \frac{dQ}{\frac{P_{\text{active}}}{N_{\text{active}}}}\right),$$

or

$$\frac{\partial n}{\partial Q} = -(P_{\text{active}}/N_{\text{active}})\frac{\partial n}{\partial x}.$$

The solution to this partial differential equation with the boundary condition of Eq. (A3) and the requirement that all particles are initially empty, is

$$\begin{array}{cc} n(Q,x) = r\,N_{\text{empty}}(Q)e^{rx} & x < x_0 \\ 0 & x > x_0 \end{array} \qquad \text{(A4)}$$

where $x_0(Q)$ is how far the boundaries nucleated at $Q = 0$ have moved when the total charge is $Q$, as given by Eq. (A2). Substituting the definitions $q_p=x/M$ and $a=r/M$ into Eq. (A4), and normalizing the probability distribution, results in Eq. (11).

**Appendix C**

Once the particles begin to become full ($x_0 = M$), the average state of charge of the active particles is

$$< x > = \int_0^M dx\, x\, n(Q,x) \,/ \int_0^M dx\ n(Q,x)$$

$$= M\left(1 - \frac{1}{Mr} + \frac{1}{e^{Mr} - 1}\right).$$

After the particles begin to become full, the total state of charge of the electrode can be written as

$$N_{\text{filled}}M \ + \ N_{\text{active}} < x > = \ Q.$$

Or, after differentiating,

$$M\ \frac{dN_{\text{filled}}}{dQ} + < x > \frac{dN_{\text{active}}}{dQ} \ = \ 1.$$

Further, because the rate of particle filling is proportional to the number of particles with state of charge near $M$, we have from Eq. (10):

$$\frac{dN_{\text{filled}}}{dQ} = -e^{rM}\frac{dN_{\text{empty}}}{dQ}.$$

With the requirement that $N_{\text{empty}} + N_{\text{filled}} + N_{\text{active}} = N$, and using $\alpha = rM$, one finds that:

$$\frac{dN_{\text{filled}}}{dQ} = \alpha\, e^{\alpha}/(e^{\alpha} - 1)$$

$$\frac{dN_{\text{empty}}}{dQ} = -\alpha/(e^{\alpha} - 1)$$

$$\frac{dN_{\text{active}}}{dQ} = -\alpha\,.$$

Integrating these equations using $N_{\text{filled}}$=0 at $Q = Q_F$ results in Eq. (12).

**References**


[1] M. E. Holtz, Y. Yu, D. Gunceler, J. Gao, R. Sundararaman, K. A. Schwarz, T. A. Arias, H. D. Abruña, and D. A. Muller, Nanoscale Imaging of Lithium Ion Distribution During In Situ Operation of Battery Electrode and Electrolyte, Nano Letters **14**, 1453 (2014).

[2] Y.-C. K. Chen-Wiegart, Z. Liu, K. T. Faber, S. A. Barnett, and J. Wang, 3D Analysis of a $LiCoO_2$–$Li(Ni_{1/3}Mn_{1/3}Co_{1/3})O_2$ Li-ion battery Positive Electrode using x-ray Nano-Tomography, Electrochem. Commun. **28**, 127 (2013).

[3] W. C. Chueh, F. El Gabaly, J. D. Sugar, N. C. Bartelt, A. H. McDaniel, K. R. Fenton, K. R. Zavadil, T. Tyliszczak, W. Lai, and K. F. McCarty, Intercalation Pathway in Many-Particle $LiFePO_4$ Electrode Revealed by Nanoscale State-of-Charge Mapping, Nano Lett. **13**, 866 (2013).

[4] J. Lim, Y. Li, D. H. Alsem, H. So, S. C. Lee, P. Bai, D. A. Cogswell, X. Liu, N. Jin, Y.-S. Yu, N. J. Salmon, D. A. Shapiro, M. Z. Bazant, T. Tyliszczak, and W. C. Chueh, Origin and Hysteresis of Lithium Compositional Spatiodynamics within Battery Primary Particles, Science **353**, 566 (2016).

[5] T. R. Ferguson and M. Z. Bazant, Phase Transformation Dynamics in Porous Battery Electrodes, Electrochim. Acta **146**, 89 (2014).

[6] P. Xiao and G. Henkelman, Kinetic Monte Carlo Study of Li Intercalation in $LiFePO_4$, ACS Nano **12**, 844 (2018).

[7] P. Bai and G. Tian, Statistical Kinetics of Phase-Transforming Nanoparticles in $LiFePO_4$ Porous Electrodes, Electrochim. Acta **89**, 644 (2013).
[8] Y. Li, F. El Gabaly, T. R. Ferguson, R. B. Smith, N. C. Bartelt, J. D. Sugar, K. R. Fenton, D. A. Cogswell, A. L. D. Kilcoyne, T. Tyliszczak, M. Z. Bazant, and W. C. Chueh, Current-induced Transition from Particle-by-Particle to Concurrent Intercalation in Phase-separating Battery Electrodes, Nat. Mater. **13**, 1149 (2014).
[9] R. M. Corless, G. H. Gonnet, D. E. G. Hare, D. J. Jeffrey, and D. E. Knuth, On the Lambert W function, Advances in Computational Mathematics **5**, 329 (1996).
[10] J. W. Christian, *The Theory of Transformations in Metals and Alloys* (Pergamon Press, Oxford, 1965).
[11] J. D. Sugar, F. El Gabaly, W. C. Chueh, K. R. Fenton, T. Tyliszczak, P. G. Kotula, and N. C. Bartelt, High-resolution Chemical Analysis on Cycled $LiFePO_4$ Battery Electrodes using Energy-filtered Transmission Electron Microscopy, J. Power Sources **246**, 512 (2014).
[12] H. Liu, F. C. Strobridge, O. J. Borkiewicz, K. M. Wiaderek, K. W. Chapman, P. J. Chupas, and C. P. Grey, Capturing Metastable Structures during High-Rate Cycling of $LiFePO_4$ Nanoparticle Electrodes, Science **344**, 1252817 (2014).
[13] X. Zhang, M. van Hulzen, D. P. Singh, A. Brownrigg, J. P. Wright, N. H. van Dijk, and M. Wagemaker, Rate-Induced Solubility and Suppression of the First-Order Phase Transition in Olivine $LiFePO_4$, Nano Lett. **14**, 2279 (2014).
[14] R. Malik, F. Zhou, and G. Ceder, Kinetics of Non-equilibrium Lithium Incorporation in $LiFePO_4$, Nat. Mater. **10**, 587 (2011).
[15] B. Orvananos, H.-C. Yu, R. Malik, A. Abdellahi, C. P. Grey, G. Ceder, and K. Thornton, Effect of a Size-Dependent Equilibrium Potential on Nano-$LiFePO_4$ Particle Interactions, J. Electrochem. Soc. **162**, A1718 (2015).
[16] B. Orvananos, H.-C. Yu, A. Abdellahi, R. Malik, C. P. Grey, G. Ceder, and K. Thornton, Kinetics of Nanoparticle Interactions in Battery Electrodes, J. Electrochem. Soc. **162**, A965 (2015).
[17] D. A. Shapiro, Y.-S. Yu, T. Tyliszczak, J. Cabana, R. Celestre, W. Chao, K. Kaznatcheev, A. L. D. Kilcoyne, F. Maia, S. Marchesini, Y. S. Meng, T. Warwick, L. L. Yang, and H. A. Padmore, Chemical Composition Mapping with Nanometre Resolution by Soft X-ray Microscopy, Nat. Photonics **8**, 765 (2014).
[18] S. Park, K. Kameyama, and T. Yao, Relaxation Crystal Analysis of $LiFePO_4$ Cathode for Li-Ion Secondary Battery, Electrochem. Solid St. Lett. **15**, A49 (2012).
[19] K. T. Lee, W. H. Kan, and L. F. Nazar, Proof of Intercrystallite Ionic Transport in $LiMPO_4$ Electrodes (M = Fe, Mn), J. Electrochem. Soc. **131**, 6044 (2009).
[20] W. Dreyer, J. Jamnik, C. Guhlke, R. Huth, J. Moskon, and M. Gaberscek, The Thermodynamic Origin of Hysteresis in Insertion Batteries, Nat. Mater. **9**, 448 (2010).

**Figures and Captions**

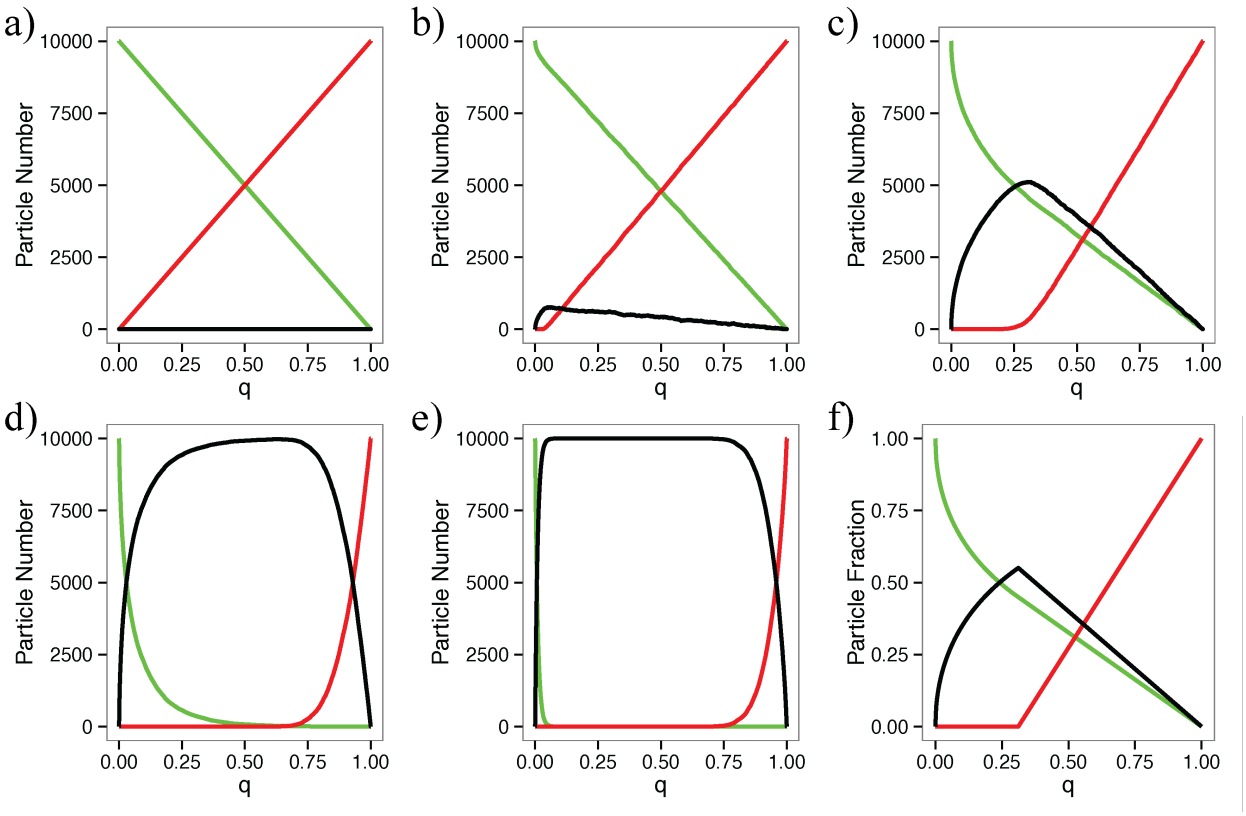


Fig. 1 (a-e) Number of active (black), filled (red) and empty (green) particles a function of the state of charge $q$ for various values of $r$, for the Monte Carlo model described in the text (for M=100). (a) $r = 8 \times 10^{-7}$, (b) $r = 8 \times 10^{-4}$, (c) $r = 8 \times 10^{-3}$ (d) $r = 8 \times 10^{-2}$, (e) $r = 1 - 10^{-6}$. To compare (c) with the analytic results, (f) plots Eq. (9) and Eq. (12) with $\alpha = rL = 0.8$.

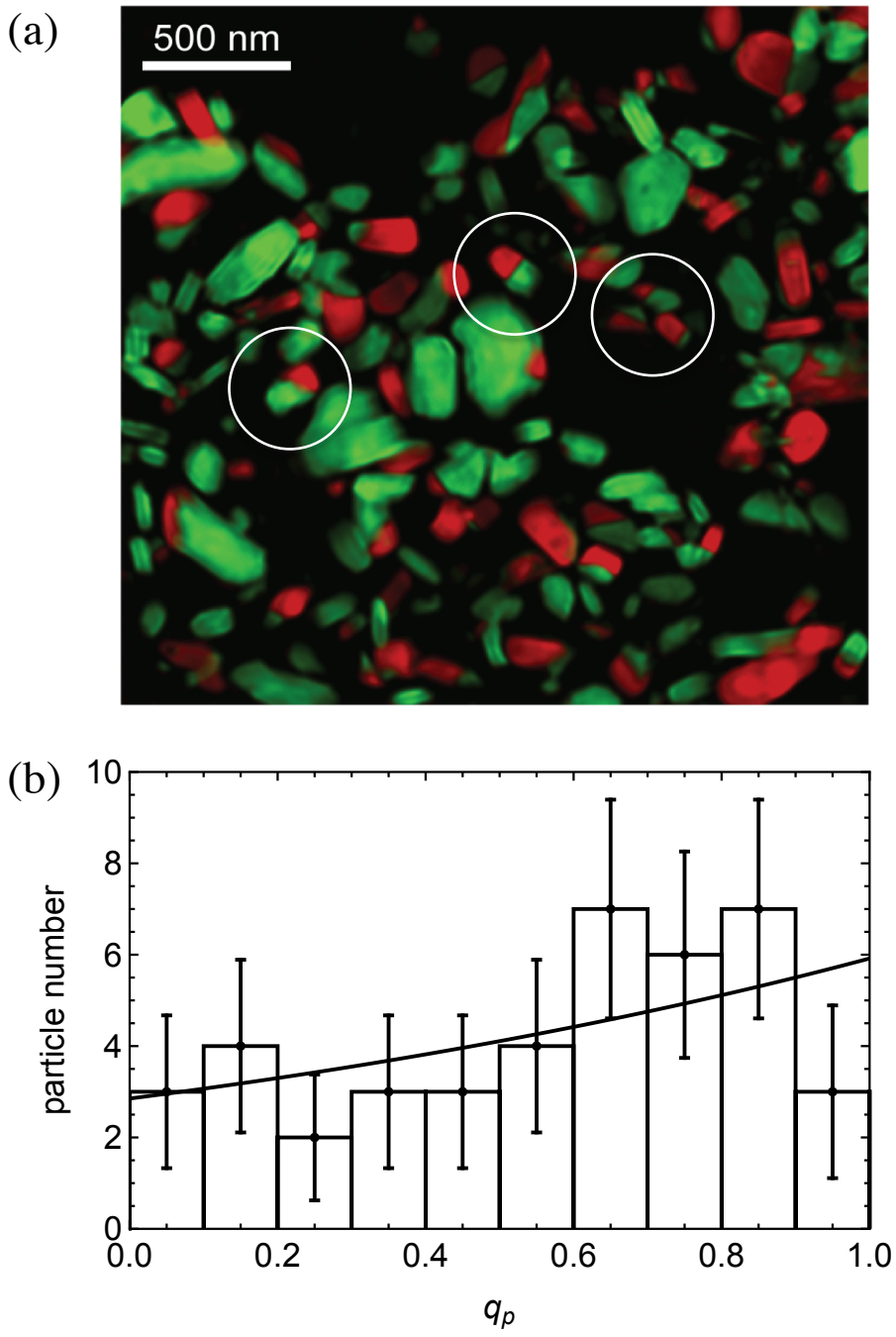


Fig. 2. (a) Ptychography STXM image of a LFP electrode at q = 42%. The green and red regions represent $FePO_4$ and $LiFePO_4$, respectively. Some examples of particles with phase boundaries are circled. (b) Histogram of the number of active particles with state-of-charge $q_p$ measured from (a). Solid line: best fit to Eq. (11), giving $\alpha = 0.73$.

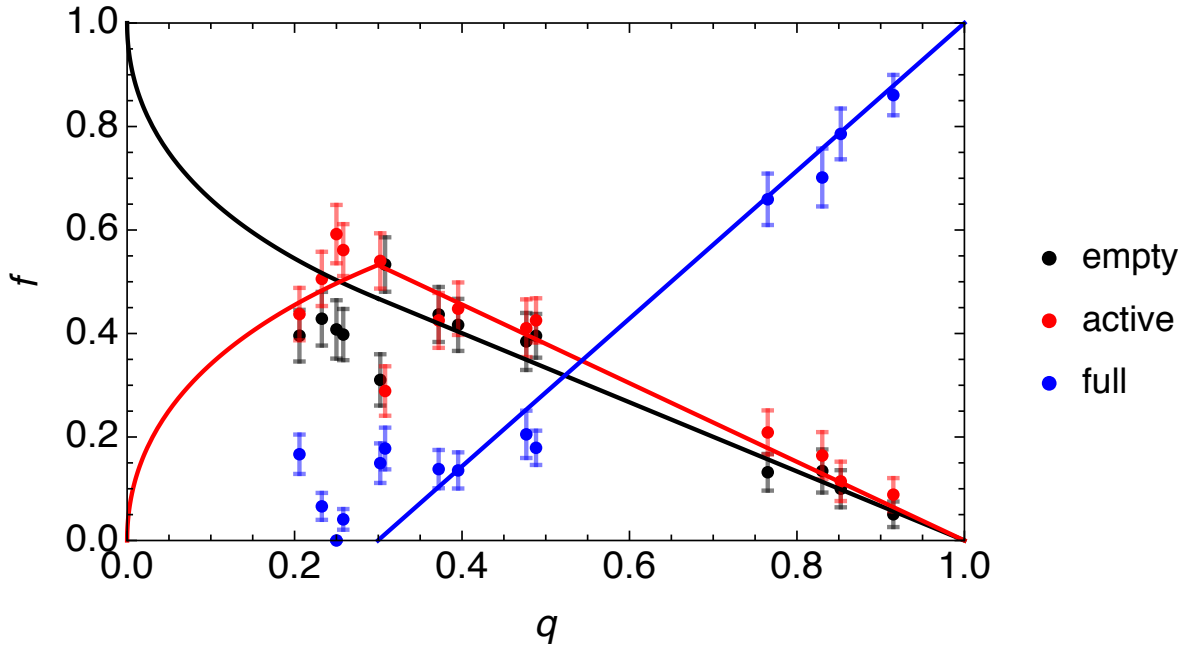


Fig. 3. Points: measured fraction, $f$, of empty, active and full particles as a function of the electrode state of charge $q$. Solid lines: best fit to Eqs. (9) and (12), giving $\alpha = 0.76$.